OPTIMIZATION OF TRANSPARENT METAL STRUCTURES BY GENETIC ALGORITHMS

Roberto Li Voti
Department of Basic and Applied Science for Engineering, Sapienza Università di Roma, via A.Scarpa 16 – 00161 Roma - Italy

Abstract

In this article the general problem of designing high performances Transparent Metal structures is deeply discussed. In particular the Genetic Algorithms are introduced as useful tool for searching the optimal thicknesses of the layers. The article deeply analyses the effect of all parameters of the Genethic Algorithms so to optimize the computational time in the optical filter design. As an example the article reviews the basic steps for the design of a particular metallo/dielectric multilayer structure made of nine layers.

Keywords: Transparent Metals, Optical Filters, Genetic Algorithms, Inverse Problems

1. Introduction

The study of novel transparent conductive coatings plays a fundamental role in the development of optical filters and devices useful in many different fields of nanotechnologies (i.e. photovoltaics, thermovoltaics, low emissivity filters, etc.). Recently a great deal of attention has been paid to the study of "*transparent metals*" which are metallo-dielectric coatings, capable to conjugate interesting and rare thermo-optical-electric properties: optical transparency, low IR emittance, radio frequency shielding, and high electrical and thermal conductance[1,2].

Transparent metals basically are 1D photonic band gap (PBG) multilayers which exhibit passband properties in the optical range. This unusual and rare property of transparency for metals is achieved by growing an adequate sequence of metal thin layers (≈10nm) and dielectric thick layers (50 ÷ 200nm). Thanks to the optical tunnelling phenomena in the metal layers, and the interference effects in the dielectric layers these structures are able to enhance the transmittance in the range of optical wavelengths only[3-5].

It is clearly understandable how the choice of the thicknesses of all these layers play a fundamental role to realise optical devices with high performances. In the following we first introduce the problem of the Transparent Metal design, showing how it can be treated as an optimization search problem; in the second part the Genethic Algorithms are introduced as an efficient tool to find the thicknesses of the layers.

Eventually all these theoretical considerations are applied to the design and realisation of real Transparent Metal structures made of nine layers.

2. Transparent Metal Design

In this paragraph the standard procedure to design a nine layers metallo/dielectric multilayer, transparent in the spectrum of wavelengths from 400 nm to 800 nm (visible window) is discussed.

Concerning the materials, as a metal the choice fell on silver (Ag) because the absorbance in the visible range is lower than for the other metals, due to the plasma resonance[6,7], at 320 nm. Titanium dioxide (TiO_2) is chosen as dielectric interlayer because it is transparent, compatible with silver, and with high refractive index[1].

An earlier study of these structures showed that a structure with n=9 layers deposited on a thick layer of glass (4 layers of silver and 5 layers of titanium dioxide. See Fig.1), might already meet the general requirements of the transparent metals[1,3,5]:

(a) to ensure a high RF shielding (30 MHz to 6 GHz) of up to 40dB. This is satisfied when the total thickness of silver is at least d_{tot} = 68nm;

(b) to show a high transparency in the visible spectrum, despite the high metal content, thanks to the optical tunneling in the thin metal layers as shown by M.Scalora et al[3].

Already with n=9, the choice of the best thickness for each layer is not trivial due to the large number of degrees of freedom of the system, so that some constraints should be introduced to reduce the free parameters, meeting the requirements (a) and (b).

The used criterion is the following: the 4 layers of silver have all the same thickness $d_{Ag}=d_{tot}/ 4$ = 17nm so to allow the optical tunneling. The 5 layers of titanium dioxide (TiO_2) are subdivided into two groups: the outer layers have all the thickness $d_{extTiO2}$, while the inner layers have all the thickness $d_{intTiO2}$ (see Fig.1). In such a way the degrees of freedom are reduced to 2, making easier the optimization in a bi-dimensional domain [$d_{extTiO2}$, $d_{intTiO2}$].

One objective of the optimization is to maximize the optical transmittance at λ= 600nm that is the central wavelength of the visible range [400nm, 800nm]. A fast optimization can be easily performed by plotting the transmittance in the 2D domain [$d_{extTiO2}$, $d_{intTiO2}$] so to start the exploration of the 2D space. As one may see from the contour lines shown in Fig.2, there are more combinations to achieve the maximum transmittance of about 88%. All those combinations have been reported with the letters A ≡ [54, 100], B≡ [178, 100], C≡ [303, 100], D ≡ [52, 224]. For a deeper understanding of the differences among all these cases, Figs.3 show the amplitude of the internal electric field in all the n=9 layers for all the structures A, B, C, and D (in abscissa is reported the order of interface. The scale for the Ag layers is expanded for clarity).

In all cases one may observe that the metal layers act as nodes of vibration for the electric field; this condition allows the optical tunneling in the metals without significant absorption, giving transparency to the whole structure.

The inner layers of TiO_2 act as resonators which exhibit an integer number m of antinodes of the electric field (see in abscissa of Figs.3 the intervals [2,3] [4,5] [6,7]). Theoretically this condition is fulfilled when the thickness of the inner layers is a multiple of half wavelength (that is $\lambda_o/2n \approx 124$ nm, where λ_o=600nm, and $n(\lambda_o)$=2.409). So for samples A,B,C where $d_{intTiO2}$=100nm there is only m=1 antinode, while for sample D, where $d_{intTiO2}$=224nm, one may observe m=2 antinodes. Deviations of thickness values from exact theory occur because the metal layers are not exactly nodes since the electric field is not zero.

Analogously in the outer layers of titanium dioxide (see the intervals [0,1] [8,9] in Figs. 3) the amplitude of the electric field should switch from high level (antinode at the TiO_2/air interface) to low level (node at the TiO_2/Ag interface) or vice versa. Ideally this is obtained when the thickness $d_{extTiO2}$ is an odd number (2k+1) of quarter wavelength ($\lambda_o/4n \approx 62$ nm). So for A and D the number of antinodes is k = 1, while for B one finds k = 2, and for C one finds k = 3.

Just to summarize the structures A, B, C, D, respond to rules similar to those of the resonators, where the modes are represented by the two indexes [k, m] which in practice represent the numbers of antinodes in each outer and inner layer, respectively.

Great differences among modes are clearly visible looking at the transmittance spectra (see Fig.4) of A,B,C,D. Although all the modes maximize the transmittance at 600nm with similar performances, they exhibit a different bandwidth of transparency in the optical range [400nm, 800nm]; in particular the higher is the mode index (B, C, D), the narrower is the bandwidth, due to the large number of oscillations related to sharp resonance conditions.

For this reason in order to evaluate the quality of transparency of any Transparent Metal structure it is helpful to introduce a parameter which compares the transmittance spectra of the filter f(λ), with the ideal objective g(λ) that is a perfect pass band filter (g(λ)=100% in the range [400nm, 800nm], and g(λ)=0 elsewhere). The distance between the two spectra is evaluated by both the *cost function* and the *fitness function* as follows

$$\cos t = \frac{\int_{\Lambda} |f(\lambda) - g(\lambda)|^2 \, d\lambda}{\int_{\Lambda} |g(\lambda)|^2 \, d\lambda} \quad , \qquad fitness = \frac{1}{\cos t^2} \tag{1}$$

where the integral in Eq.(1) is calculated in the extended domain $\Lambda \equiv$ [300nm, 900nm]; by definition the *cost function* reaches its minimum value (zero) only if the transmittance spectra of the Transparent Metal f(λ) coincides with the objective function g(λ). This desirable condition corresponds to the maximum of the *fitness function,* and represents the optimal structure.

Figs.5 show the contour plots for the *cost function* (fig.5a) as well as for the *fitness function* (fig.5b) in the same 2D domain [$d_{extTiO2}$, $d_{intTiO2}$] of Fig.2. The *cost function* exhibits in fig.5a a series of local minima (i.e. optimal structures) almost correspondent to the modes already discussed in Fig.2. The absolute minimum of cost≈0.23 (fitness≈18) is reached for the optimal structure [$d_{extTiO2}$=34nm, $d_{intTiO2}$=72nm] not too far from the mode A [k=1, m=1].

As a conclusion this simple example demonstrates how important is:

a) to identify the objective function g(λ) capable to achieve the requirements;
b) to introduce quantitative functions like *cost* and *fitness* useful for the optimization procedure;
c) to find tools to explore the domain of the "*layer thicknesses"*, and find the minimum of the cost function. In the previous example this domain is only 2D and has been explored by contour plots.

3. Optimization of the Transparent Metal Design by Genetic Algorithms

The previous paragraph clarifies how the procedure to design a "*transparent metal*" structure basically consists in the minimization of the *cost function* (maximization of the *fitness function*) as described in Eq.(1).

In this paragraph Genetic Algorithms are introduced as a tool for a quick inspection of the domain of the "*layer thicknesses",* and for a fast detection of the absolute minimum of the *cost function,* even in multidimensional research domains.

Genetic Algorithms (GA) have been introduced in the 60s by John Holland and his group at University of Michigan for two purposes: to explain the adaptive processes of natural systems, and to design artificial systems software capable to emulate the mechanisms of natural systems[8,9]. In the following years GA have been applied to solve both optimization and inverse problems in many different scientific fields: in biology to simulate the evolution of single celled organism populations[10,11], in computer science for the parallel implementation on Intel hardware[12], in engineering and physics for recursive adaptive filter design[13], in for optimization of gas pipeline[14], for the VLSI circuit layout[15], for aircraft landing strut weight optimization[16], for communications network link size optimization[17], for seismic inversion problems[18], for inverse problem in synthesis of fiber gratings[19], for local search for thin film metrology[20], in image processing, for image registration via GA to minimize image differences[21], to search for image feature detectors via GA[22], for hardness depth profiling in hardened steels with photothermal radiometry[23-26]

The mechanic of the GA is always surprisingly simple. Adopting the terminology of the biological sciences, the *chromosome* is an *individual* that represents a possible solution in the research space. In the previous paragraph the 2D research domain is given by the couple $[d_{ext\ TiO2}\ ,\ d_{int\ TiO2}]$, so that the chosen *chromosome* is an array with 2 components (2 genes) representing the thicknesses of the outer and inner titania layers respectively. According to this terminology, for example the *chromosome* v = [188, 93] represents the Transparent Metal structure obtained with $d_{extTiO2}$=188nm and $d_{intTiO2}$=93nm. Each *chromosome* identifies a specific *individual* who belongs to the *population* of N_{pop}=16 individuals. As a result of mutual interactions among individuals, the population can evolve and adapt to the environment (research domain).

Table 1 shows the initial population of N_{pop}=16 individuals. The genes of each individual are initially randomly chosen in the intervals $0<d_{extTiO2}<200$, and $0<d_{intTiO2}<200$ and reported in columns 2 and 3, Both fitness and cost functions are reported respectively in columns 4, and 5. The individuals are sorted in descending order of fitness, so that the best individuals can be found at the top of the list. The *selectivity function* is also introduced in column 6. Selectivity represents the probability of one particular individual to be randomly selected for the *reproduction* so to transfer its *chromosomic string* to future generations. According to GA philosophy, selectivity is simply chosen proportional to the fitness, so to drive the random selection giving more chances for reproduction to the best individuals respect to the worst ones that risk the extinction.

This selection process is well documented in Table 2, where, after a random selection of the initial population, 8 couples are formed for reproduction. It is worth noting that the best individuals can be selected more than once as happens for individual [142, 75] who is selected three times in Table 2 (No.5, No.6, No.11) since in Table 1 he was at the top of the list (No.2).

The reproduction process begins after that the selected individuals are grouped into $N_{pop}/2$=8 couples. Each parent couple (X, Y) generate two sons (S_1, S_2) with the mechanism shown in Table 3. The genes of sons are obtained by a weighted average of the parental genes according to the following rule

$$S_1 = X \cdot j + Y \cdot (1 - j) \qquad \text{(Son 1)}$$
$$S_2 = X \cdot k + Y \cdot (1 - k) \qquad \text{(Son 2)}$$

where j and k are numbers randomly chosen in the interval [0, 1].

After reproduction a new population of children is generated, which should have an average fitness better than the previous one, thanks to the selection rules and to the general assumption that good parents generate good children. In synthesis the new generation tends to adapt more to the environment.

But sometimes it happens that after several generations, the individuals become too similar to each other. This dangerous phenomenon may produce an evolutionary stop (epistasis) which inhibits further improvement of the population. To avoid the *epistasis,* a random mechanism of *mutation* of the genes should be introduced. Accordingly each single gene may be mutated and substituted by a random value in the same range [0, 200], but this may happen only with a small probability (typically p_m = 5%). This mutation creates a new individual, sometimes extremely different from its parents, but anyway useful for the renewal of the population. For example in Table 4, the individual No.1 has been subjected to the mutation of the second gene, generating by chance a better individual.

Last mechanism of GA is the *elitism*, which allows to clone the best individual and keep it unchanged for the next generation. Therefore e*litism* avoids the regression of the evolutionary process that might statistically occur.

In conclusion Table 4 summarizes the population of the second generation after the whole procedure of selection, reproduction, mutation, elitism and sorting by fitness.

Fig. 6 shows the initial population (first generation) made of 16 individuals randomly chosen (symbols □) together with the second generation (symbol ●). From the contour lines of the fitness function one may see a general improvement of the second generation respect to the first one, thanks to the GA postulate. Figs. 7 show, with more details, the improvements from the 5th (fig.7a) to the 44th generation (fig.7b), demonstrating how the population collectively moves towards the absolute maximum of the fitness (≈18). The evolution of the best individual is shown generation by generation in Fig.8; from this graph a quasi optimal solution around [35, 72] has already reached already after 5 generations. Additional improvements, still visible up to 38^{th} generation, are convergent towards the absolute maximum around [34, 72]. Finally Fig.9 shows the transmittance spectra of the best individual at some generations (at 1st, 2nd, 5th, 38th, and 50^{th} generation). As one may see the improvements in the transmittance spectra from generation 38^{th} to generation 50^{th} are hardly recognized, and in practice the transmittance is already optimized before the 38^{th} generation!

One fundamental question is now how the evolutionary process can be speeded up so to reduce the computation time needed for finding the optimal Transparent Metal structure. One way may be obtained by reducing the size of the population N_{pop} so to lower its inertia, making faster the collective movements of the population towards the local maximum of fitness. A simple comparison on the performance of GA by changing N_{pop} is shown in Fig. 10a; the cost function of the best individual is here plotted as a function of the number of generation. Each curve refers to a particular value of N_{pop} (6, 16, 20) and has been selected over a large set of curves obtained by running 10 times the GA with different initial conditions. By a first inspection of Fig,10a the choice of the small value N_{pop}=6, on one hand guarantees the quickest computational time to find the local maximum of fitness (minimum of cost), but, on the other hand makes the population poor of individuals (poor complexity) preventing the exploration of the research domain, and failing to find the absolute maximum otherwise obtained for N_{pop}=16 or 20. Obviously for each particular problem of optimization there is an optimal size of the population N_{pop}

(connected to the degrees of freedom/genes) which conjugates the right complexity with the reasonable computational time to find the best solution (in our case N_{pop}=16).

An analogous study can be done by changing the probability of mutation p_m of the GA in the range [1%,10%]. Even in this case an optimal value of p_m exists that is able to speed up the evolutionary process. Fig.10b shows the cost function of the best individual vs the number of generation (computational time) for different values of p_m (1%, 5%, 10%). On one hand the choice of low values of p_m (1%) inhibit the mutation, increasing the risks of epistasis which slows down the research in the domain. On the other hand, the choice of large values of p_m (10%), due to the continuous mutation of genes, are particularly indicated for a quick initial search in large domains rather than for an accurate final search when at last the domain has been restricted. Fig.10b shows that a trade off of these different features is obtained for the optimal value of p_m=5%.

In the previous part Genetic Algorithms are used to optimize the choice of two parameters (2D) which represent the outer and inner layers of titania (respectively $d_{extTiO2}$ and $d_{intTiO2}$). But GA are much more powerful and can be applied for the optimization of all the layers of the Transparent Metal simultaneously: in our case the 5 layers of titania and the 4 layers of silver, with or without the additional constraint on the total thickness of silver (d_{tot}=68nm). With this large number of degrees of freedom (8D or 9D) the optimal size of the population becomes N_{pop} = 20, the optimal probability of mutation is p_m = 5.5%, while the expected number of generations to find a solution can easily reach the value of one thousand.

In the particular case of 8 degrees of freedom (with the constraint of a fixed total amount of silver d_{tot}=68nm), after about 1000 generations, the Genetic Algorithms, here called GA_{8D}, converge towards an optimal solution not really different from the one already explored in Figs.8 and 9 where GA_{2D} used 2 degrees of freedom only. Figs.11 show at each generation the thicknesses of the layers for the best individual. As one can see the thicknesses of the layers of silver (Fig.11b) substantially don't differ each other, while the thicknesses of titania (Fig.11a) tend to split spontaneously into two groups: the outer layers (No.1 and No.5) and the inner layers (No.2, No.3, and No.4). As told before, the *chromosomic string* obtained after thousands of generations [34, 19, 73, 16, 70, 16, 73, 17, 34] is very similar to simple one shown in Fig.9 [34, 17, 72, 17, 72, 17, 72, 17, 34]. Consequently the transmittance spectra is only marginally improved.

In the particular case of 9 degrees of freedom (without any constraint on the amount of silver) the Genetic Algorithms, here called GA_{9D}, are able to improve substantially the fitness. Fig.12 shows how the performances of GA_{9D} are much better with respect with GA_{8D} and GA_{2D} . In particular after 1000 generations the fitness of GA_{9D} reaches the value of 100. Fig. 13 shows the evolution of the transmittance spectra obtained with GA_{9D} after 100, 200, 500, 1000, 2000 generations. By comparing the GA_{9D} final spectra in Fig.13 with GA_{2D} final spectra in Fig.9, the bandwidth of the Transparent Metal is clearly increased according to the requirements defined by the ideal objective filter.

Figures 14 eventually show the thicknesses of the titania layers (Fig.14a) and of the silver layers (Fig.14b) as a function of the order of generation. The graphs become stable after about 1000 generations giving rise to the optimal Transparent Metal structure [32, 14, 63, 12, 62, 11, 64, 11, 33]. Again note how the thicknesses of the titania layers tend to split spontaneously in the same two groups as below. Note also that the average transparency of the structure is increased because the total amount of silver decreases to about 48nm.

4. Conclusions

In this article the general problem of the design of high performances Transparent Metal structures is deeply discussed. It is also shown how Genethic Algorithms represent useful tool for searching for the optimal thicknesses of the layers. All the theoretical considerations have been applied for the design of Transparent Metal structure made of 5 layers of titania and 4 thin layers of silver, but obviously the same method can be extended to any multilayer structure.

5. Acknowledgments

The author is indebted with S. Gaetani for very useful discussions.

6. References

[1] M.S.Sarto, R. Li Voti, F. Sarto, M.C. Larciprete, IEEE Transactions on Electromagnetic Compatibility 47, 602-611 (2005).
[2] M. C. Larciprete, C. Sibilia, S. Paoloni, M. Bertolotti, F. Sarto, and M. Scalora, *J. Appl. Phys.*, vol. 93, p.5013–5017, (2003).
[3] M. Scalora,M. J. Bloemer,A. S.Manka, S.D. Pethel, J. P. Dowling, and C.M. Bowden, *J. Appl. Phys.*, vol. 83, pp. 2377–2383, 1998.
[4] M.J.Bloemer and M.Scalora, Appl. Phys. Lett. 72, 1676 (1998);
[5] M. Scalora, M.J. Bloemer, and C.M. Bowden, Opt. Photon. News 10 p.23 (1999);
[6] W. Steinmann, Phys. Rev. Lett. 5, 470–472 (1960);
[7] M. Bender, W. Seelig, C. Daube, H. Frankeberger, B. Ocker, and J. Stollenwerk, *Thin Solid Films*, vol. 326, pp. 67–71, 1998.
[8] Holland, J.H.,*Journal of the Association for computing machinery*, 3, 297-314 (1962)
[9] Holland, J.H., *Adaptation in natural and artificial systems*.
Ann Arbor: The University of Michigan Press
[10] Rosenberg R.S., *Mathematical Biosciences* 7, 223-257 (1970)
[11] Rosenberg R.S., *Mathematical Biosciences* 8, 1-37 (1970)
[12] Pettey, C.B., Leuze M.R., GrefenstetteJ.J., *Second international conference on genetic algorithms* 151-161 (1987)
[13] Etter, D.M., Hicks M.J., & Cho K.H., IEEE International conference on acoustics, speech and signal processing, 2, 635-638 (1982)
[14] Goldberg D.E*., Dissertation Abstracts International* 44 (10) 3174b (1983)
[15] Davis, L., *Adaptive design for layout synthesis*, Texas Instrument report. Dallas (1985)
[16] Minga A.K., presented at AIAA Southeastern Regional Student Conference, Huntsville, (1986)
[17] Davis, L., *Genetic Algorithms and simulated annealing*, London: Pitman(1987)
[18] Sushil, J.L., Li Li Serdar Ozalaybey, Genetic Algorithms for seismic travel-time inversion
[19] Skaar J., Risvik K.M., Journal of lightwave technology 16, 1928-1932 (1998)
[20] Lienert B..R., Porter J.,N., Sharma S., K., Applied Optics 40, 3476-3482 (2001)
[21] Fitzpatrick J.M., Grefenstette J.J., & Van Gucht, D., IEEE southeast conference 460-464 (1984)
[22] Gillies A.M., *Machine learning procedures for generating image domain feature detectors. Doctoral dissertation*. University of Michigan (1985)
[23] R. Li Voti in Advances in Signal Processing for Nondestructive Evaluation of Materials, Vol.6 Ed. X:Maldague, ASNT, p.31 (2002)
[24] R. Li Voti, C. Melchiorri, C. Sibilia, M. Bertolotti, Analytical Sciences 17 p.410 (2001)

[25] R. Li Voti, C.Sibilia, M. Bertolotti, Rev.Sci. Instrum. vol. 74, p. 372 (2003).
[26] R. Li Voti, C.Sibilia, M.Bertolotti, International Journal of Thermophysics 26 p.1833 (2005).

Caption for figures

Figure 1: Sketch of the Transparent Metal structures.

Figure 2: Contour plot of the optical transmittance at λ=600nm as a function of the thickness of the outer layers $d_{extTiO2}$. and inner layers $d_{intTiO2}$ of Titanium dioxide. The letters A, B, C, D, identifies some local maxima.

Figures 3: Amplitude of the internal electric field at the wavelength 600nm in the nine layers of the structure: (a) comparison between samples A. B; (b) comparison between samples C. D. The size of the Silver layers is expanded for clarity.

Figure 4: Transmittance spectra in the range of wavelengths [300nm-900nm] for the different samples A, B, C, D

Figures 5: contour plots of the *cost function* (a) and of the *fitness function* (b) in the 2D domain of $d_{extTiO2}$ and $d_{intTiO2}$ that are the thicknesses of the outer and inner layers of titania;

Figure 6: Map of the population in 2D domain [$d_{extTiO2}$,$d_{intTiO2}$] at the fist (□) and second (●) generation. Symbols are used to localize the individuals in the research domain.

Figure 7: Magnified map of the population in the 2D domain [$d_{extTiO2}$,$d_{intTiO2}$]: (a) at the 5^{th} generation; (b) at the 44^{th} generation. Symbols (●) are used to localize the individuals in the research domain.

Figure 8: Map in 2D domain [$d_{extTiO2}$,$d_{intTiO2}$] of the best individual of the population at the generations 2^{nd}, 5^{th} 21^{st}, 29^{th}, 38^{th} .

Figure 9: Transmittance spectra of the best individual of the population at at the generations 1^{st} 2^{nd}, 5^{th} , 38^{th} , 50^{th} .

Figures 10: Cost function and Fitness function vs order of generation: (a) the curves refer to different values of the size of the population N_{pop} ; (b) the curves refer to different values of the probability of mutation p_m.

Figures 11: Evolution of the optimized thickness vs the order of generation for GA_{8D}: (a) thickness of the 5 layers of titania; (b) thickness of the 4 layers of silver;

Figure 12: Comparison among cost and fitness functions vs order of generation. The curves refer to the different Genetic Algorithms GA_{2D}, GA_{8D}, GA_{9D}, respectively with 2, 8 and 9 degrees of freedom.

Figure 13: Transmittance spectra calculated by GA_{9D} for the best individuals at generation 100^{th} , 200^{th} , 500^{th} , 1000^{th} , 2000^{th}

Figures 14: Evolution of the optimized thickness vs the order of generation for GA_{9D}: (a) thickness of the 5 layers of titania; (b) thickness of the 4 layers of silver;

Caption for Tables

Table 1: Summary of the initial population (first generation) of the Genetic Algorithms GA_{2D}. Column 1; priority order; column 2: gene $d_{extTiO2}$; column 3: gene $d_{intTiO2}$; column 4: fitness function; column 5: cost function: column 6: probability of selection.

Table 2: Mechanism of selection of the individuals reported in Table 1

Table 3: Mechanism for coupling of the couple No.1 reported in Table 2.

Table 4: Summary of the second generation of the Genetic Algorithms GA_{2D}. Column 1; priority order; column 2: gene $d_{extTiO2}$; column 3: gene $d_{intTiO2}$; column 4: fitness function; column 5: cost function: column 6: probability of selection.

N°	$d_{extTiO2}$	$d_{intTiO2}$	Fitness	Cost	Selectivity
1°	188.1	93.1	4.69	0.46177	11.77%
2°	143.5	75.3	4.66	0.46300	11.71%
3°	121.9	67.1	3.80	0.51303	9.54%
4°	193.3	111.6	3.56	0.52995	8.94%
5°	79.7	106.0	2.80	0.59763	7.03%
6°	161.8	189.9	2.70	0.60832	6.78%
7°	129.9	90.0	2.45	0.63918	6.15%
8°	49	125.6	2.20	0.67475	5.51%
9°	97.5	124.6	2.06	0.69728	5.16%
10°	1.4	112.9	2.02	0.70286	5.08%
11°	191.6	140.2	1.79	0.74812	4.49%
12°	50.9	162.9	1.76	0.75310	4.43%
13°	61.1	161.4	1.48	0.82336	3.70%
14°	190.7	157.2	1.47	0.82429	3.70%
15°	89.3	151.5	1.22	0.90527	3.06%
16°	80.7	17.4	1.17	0.92432	2.94%

Table 1

N°	$d_{extTiO2}$	$d_{intTiO2}$	Old N°	Couple
1)	129.9	90.0	7°	1
2)	49.0	125.6	8°	
3)	89.3	151.5	15°	2
4)	161.8	189.9	6°	
5)	143.5	75.3	2°	3
6)	143.5	75.3	2°	
7)	1.4	112.9	10°	4
8)	49.0	125.6	8°	
9)	193.3	111.6	4°	5
10)	1.4	112.9	10°	
11)	143.5	75.3	2°	6
12)	97.5	124.6	9°	
13)	121.9	67.1	3°	7
14)	89.3	151.5	15°	
15)	97.5	124.6	9°	8
16)	121.9	67.1	3°	

Table 2

	Parents		Sons	
N°	**$d_{extTiO2}$**	**$d_{intTiO2}$**	**$d_{extTiO2}$**	**$d_{intTiO2}$**
1)	129.9	90.0	101.4	109.9
2)	49.0	125.6	62.0	119.3

j_1=0.648	**j_2=0.441**
X_{11}=129.9	X_{12}=90.0
Y_{11}=49.0	Y_{12}=125.6
S_{11}=129.9*0.648+49.0*(1-0.648)=**101.4**	**S_{12}**=90.0*0.441+125.6*(1-0.441)=**109.9**
k_1=0.161	**k_2=0.177**
X_{21}=129.9	X_{22}=90.0
Y_{21}=49.0	Y_{22}=125.6
S_{21}=129.9*0.161+49.0*(1-0.161)=**62.0**	**S_{22}**=90.0*0.177+125.6*(1-0.177)=**119.3**

Table 3

N°	$d_{extTiO2}$	$d_{intTiO2}$	Fitness	Cost	Selectivity
1°	35.6	**68.4**	13.1532	0.28	23.77%
2°	**188.1**	**93.1**	4.68978	0.46	8.48%
3°	143.5	75.3	4.66491	0.46	8.43%
4°	143.5	75.3	4.66491	0.46	8.43%
5°	121.3	69.0	3.69587	0.52	6.68%
6°	91.2	70.3	2.53808	0.63	4.59%
7°	103.8	112.2	2.52022	0.63	4.56%
8°	14.8	111.7	2.49074	0.63	4.50%
9°	114.2	84.6	2.47740	0.64	4.48%
10°	107.4	86.0	2.38645	0.65	4.31%
11°	112.3	86.3	2.36972	0.65	4.28%
12°	140.2	181.7	2.35029	0.65	4.25%
13°	62.0	119.3	2.32723	0.66	4.21%
14°	106.9	95.5	2.20920	0.67	3.99%
15°	48.5	31.4	1.47359	0.82	2.66%
16°	96.3	156.2	1.31313	0.87	2.37%

Table 4

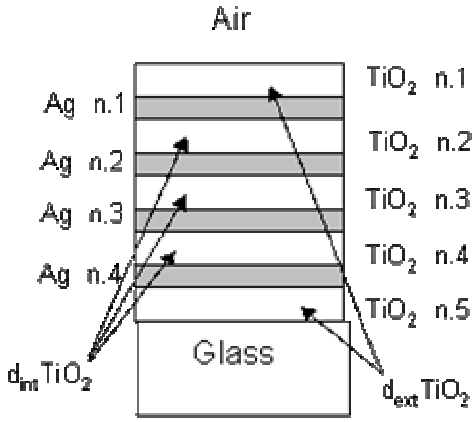

Fig.1 - R. Li Voti

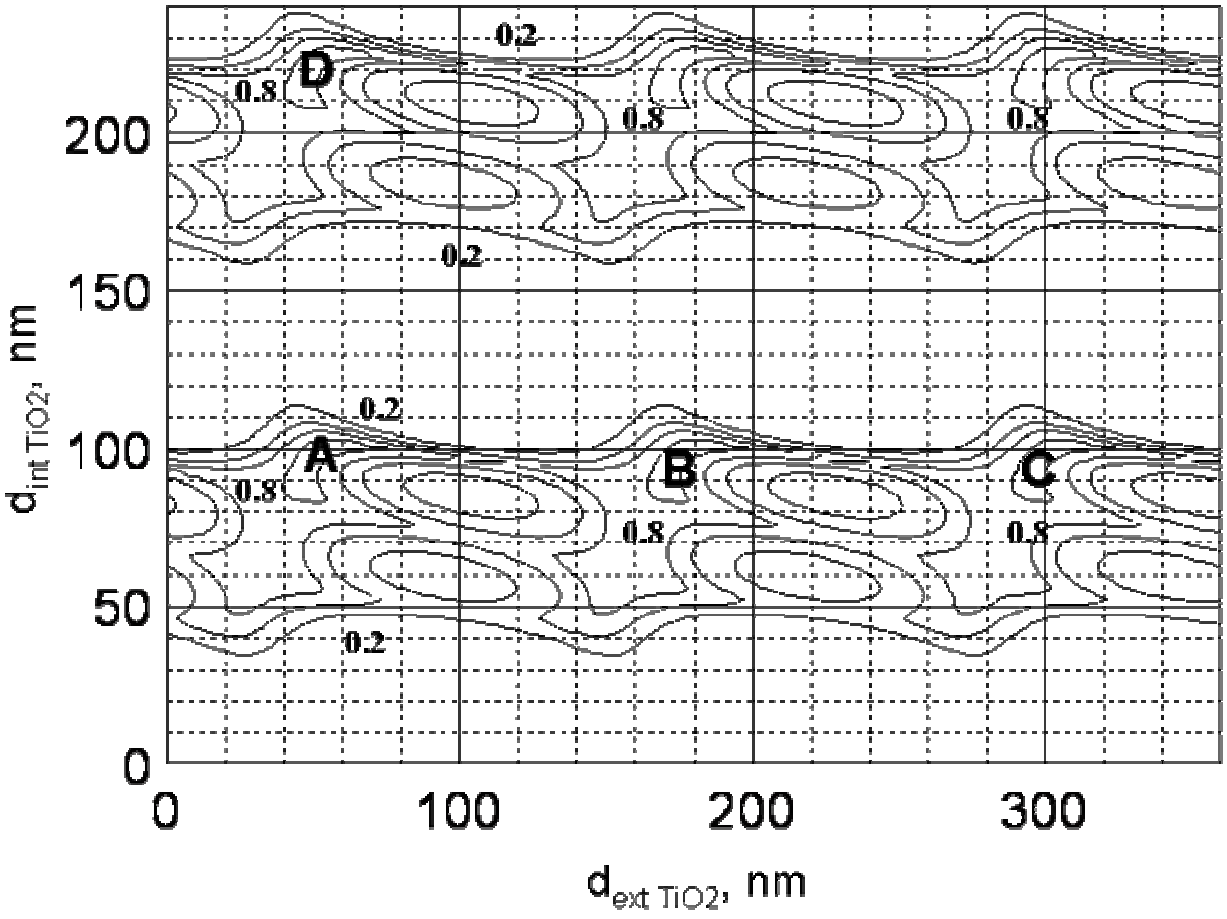

Fig. 2 - R. Li Voti

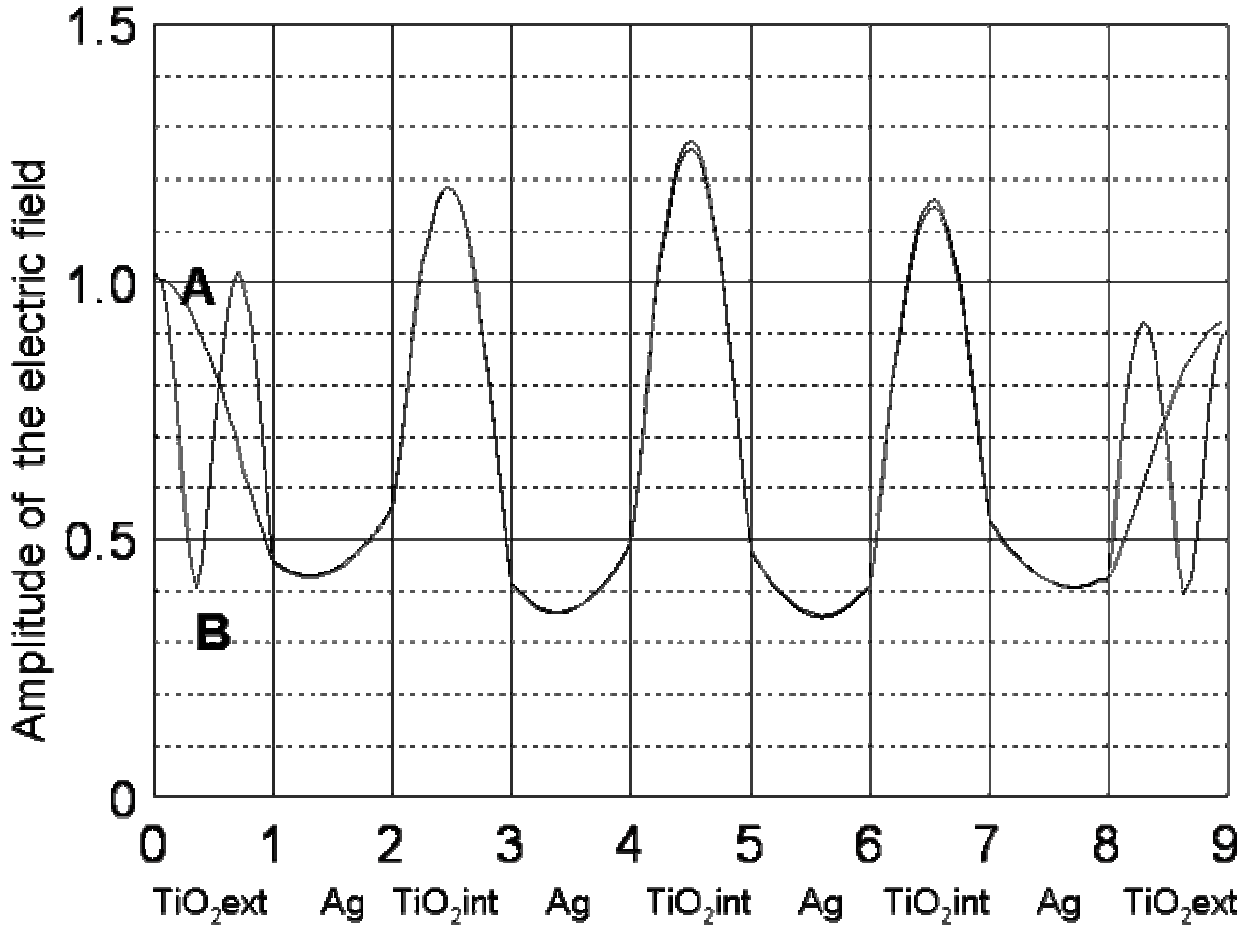

Fig. 3a - R. Li Voti

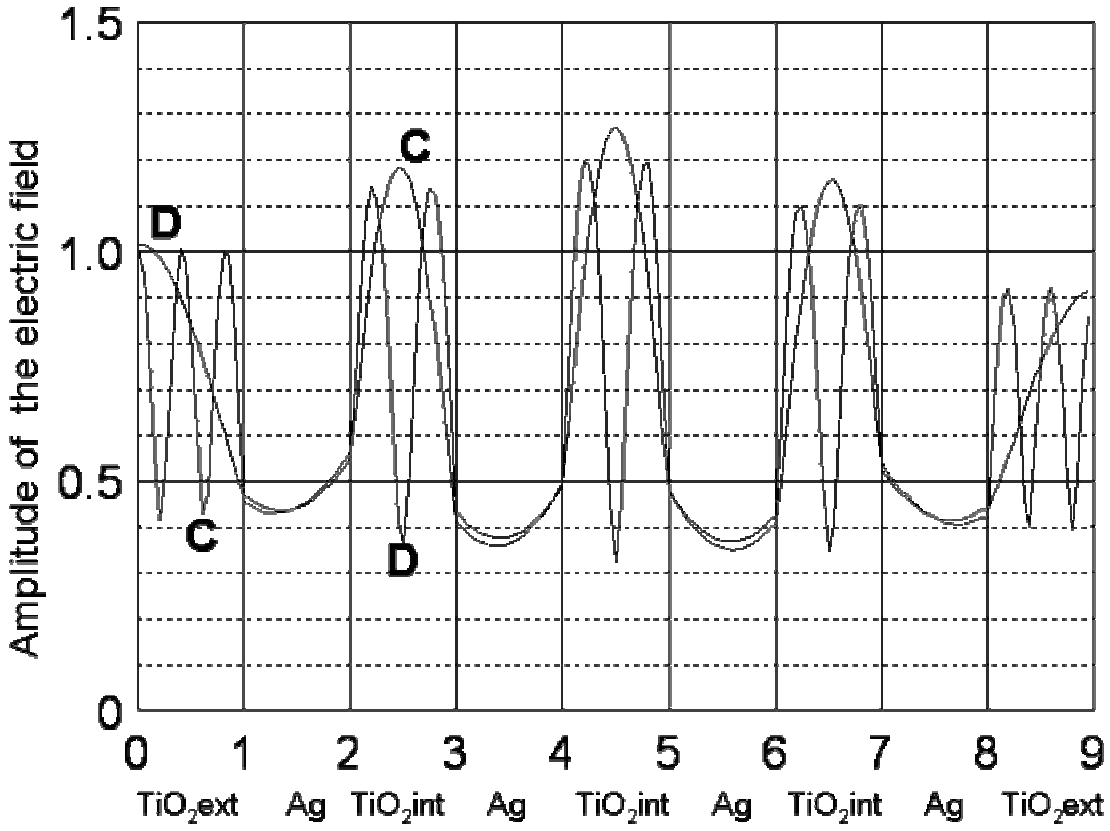

Fig. 3b - R. Li Voti

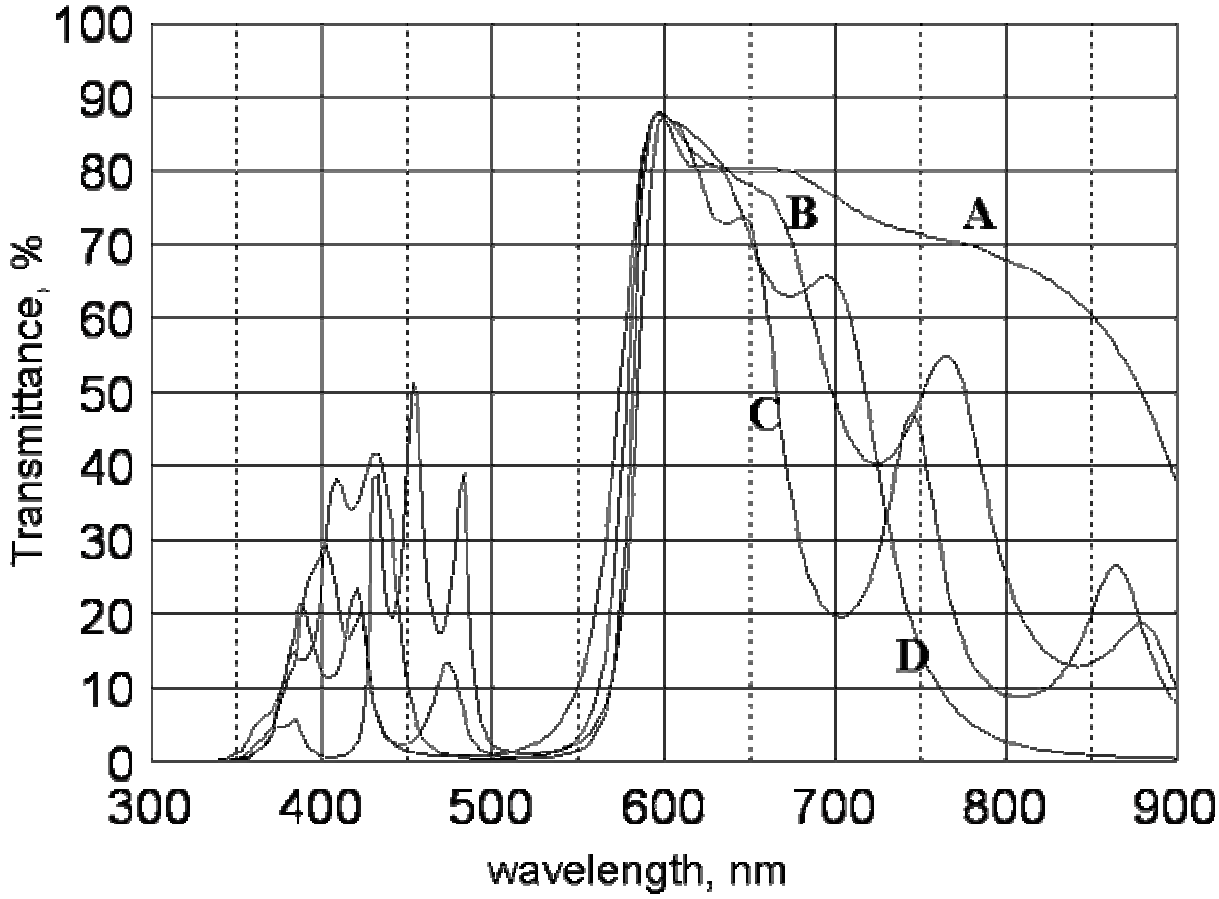

Fig. 4 - R. Li Voti

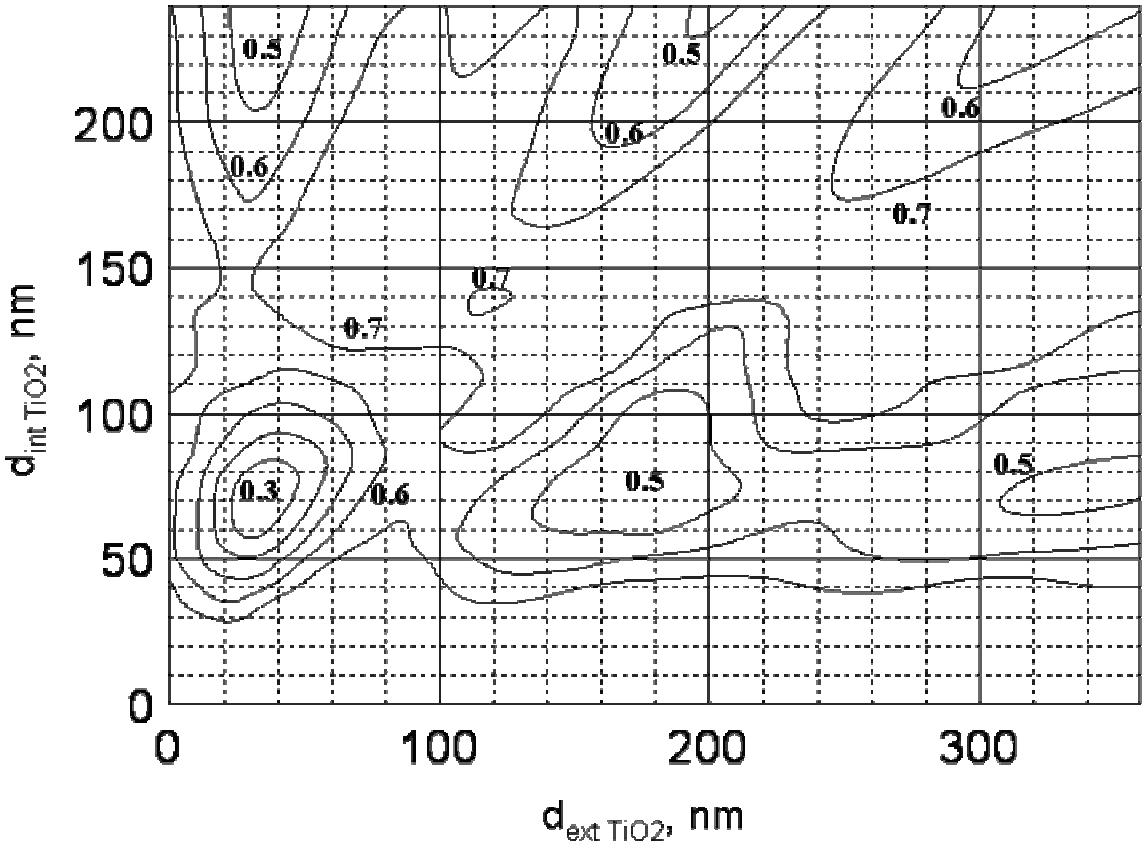

Fig. 5a - R. Li Voti

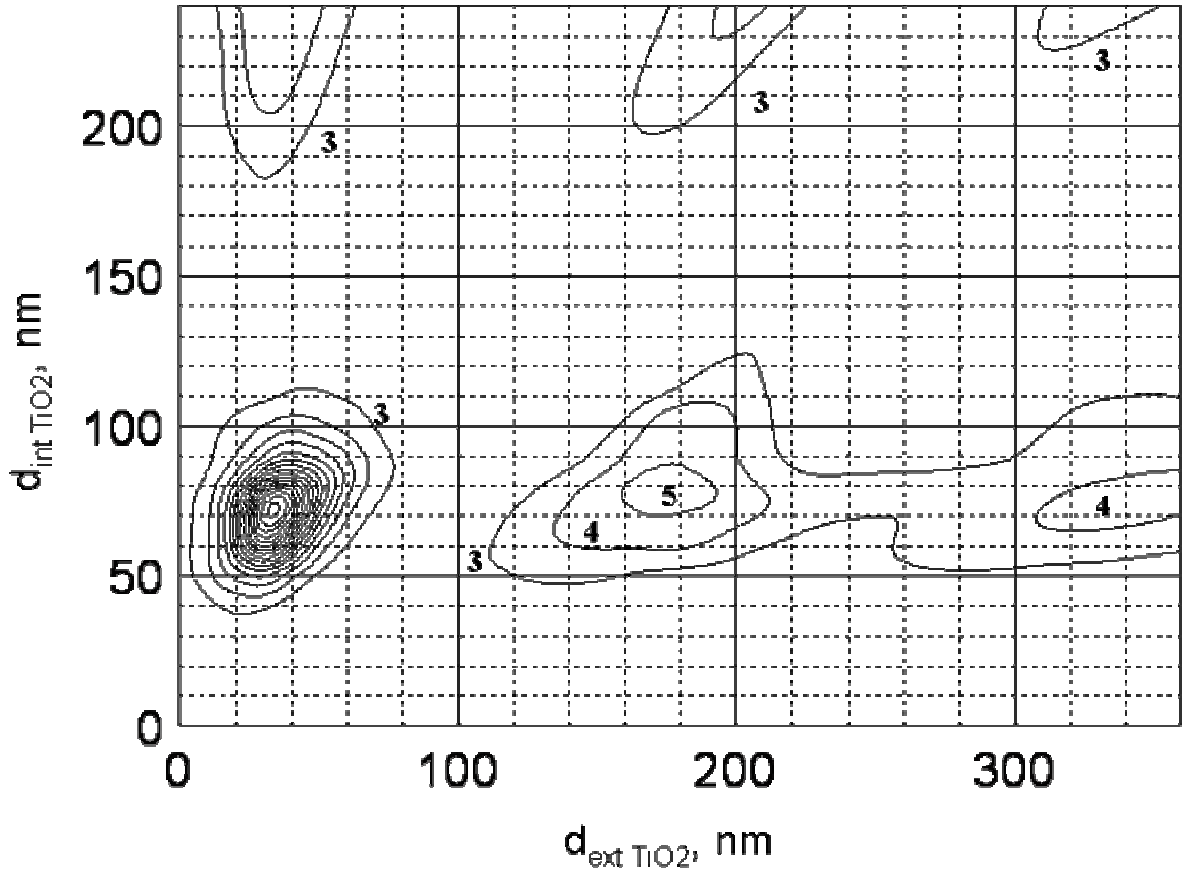

Fig. 5b - R. Li Voti

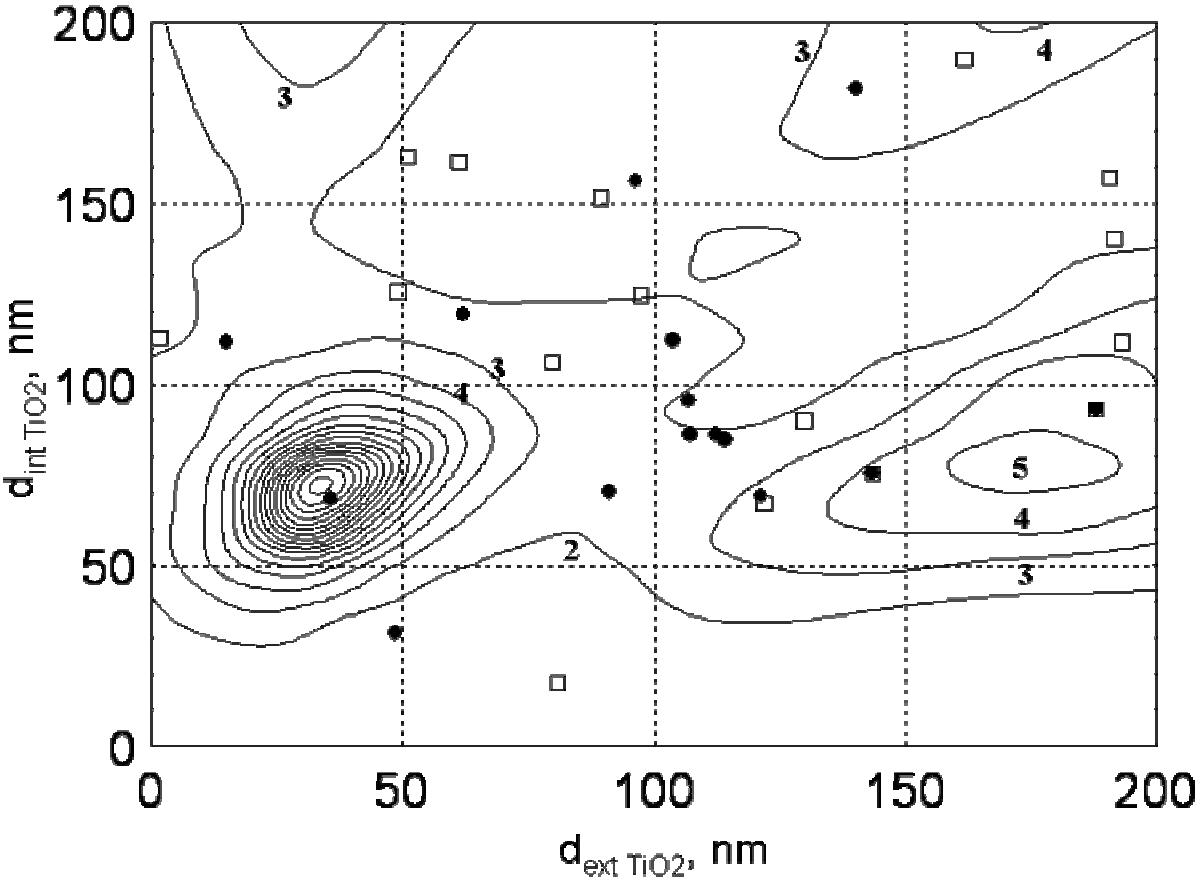

Fig. 6 - R. Li Voti

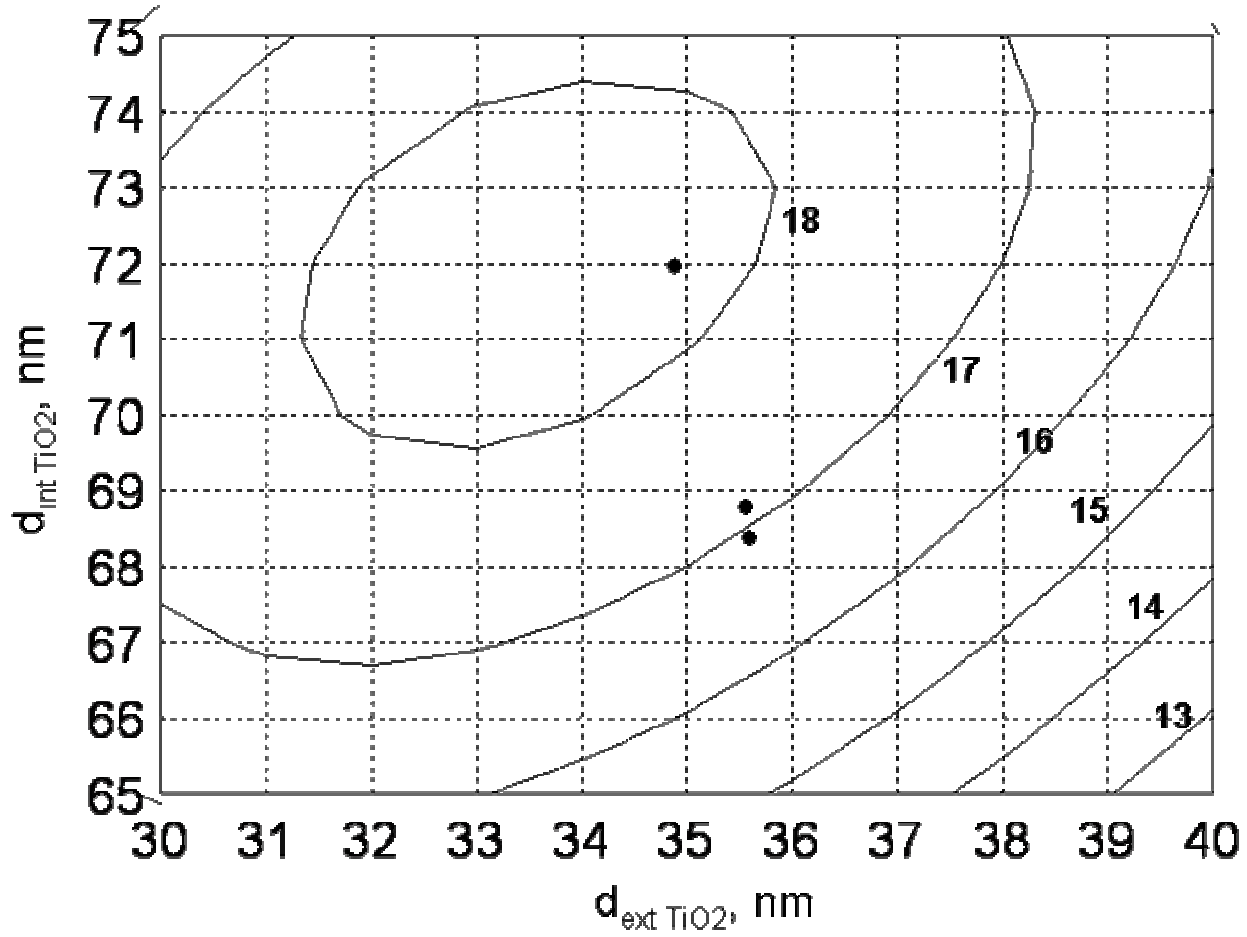

Fig.7a - R. Li Voti

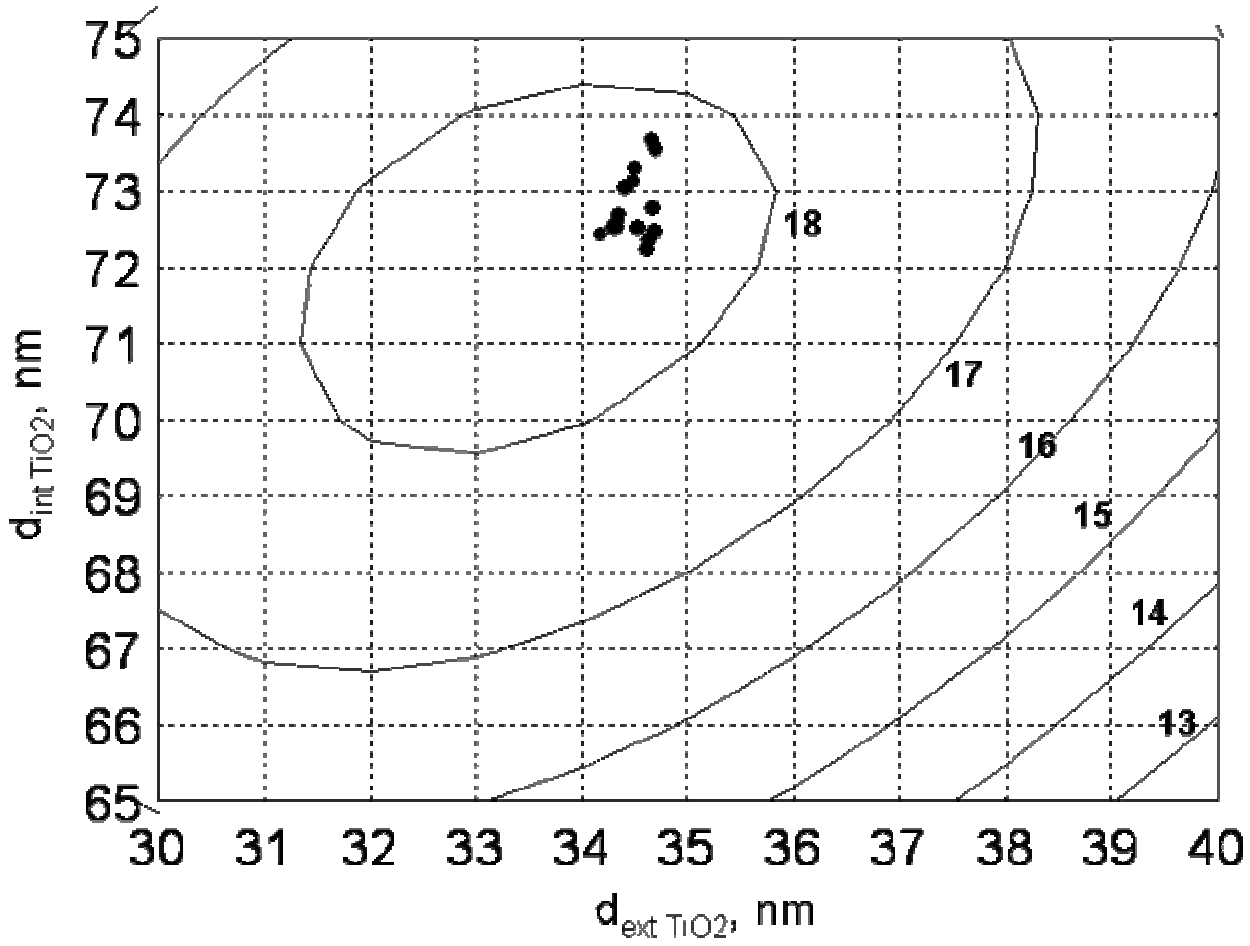

Fig. 7b - R. Li Voti

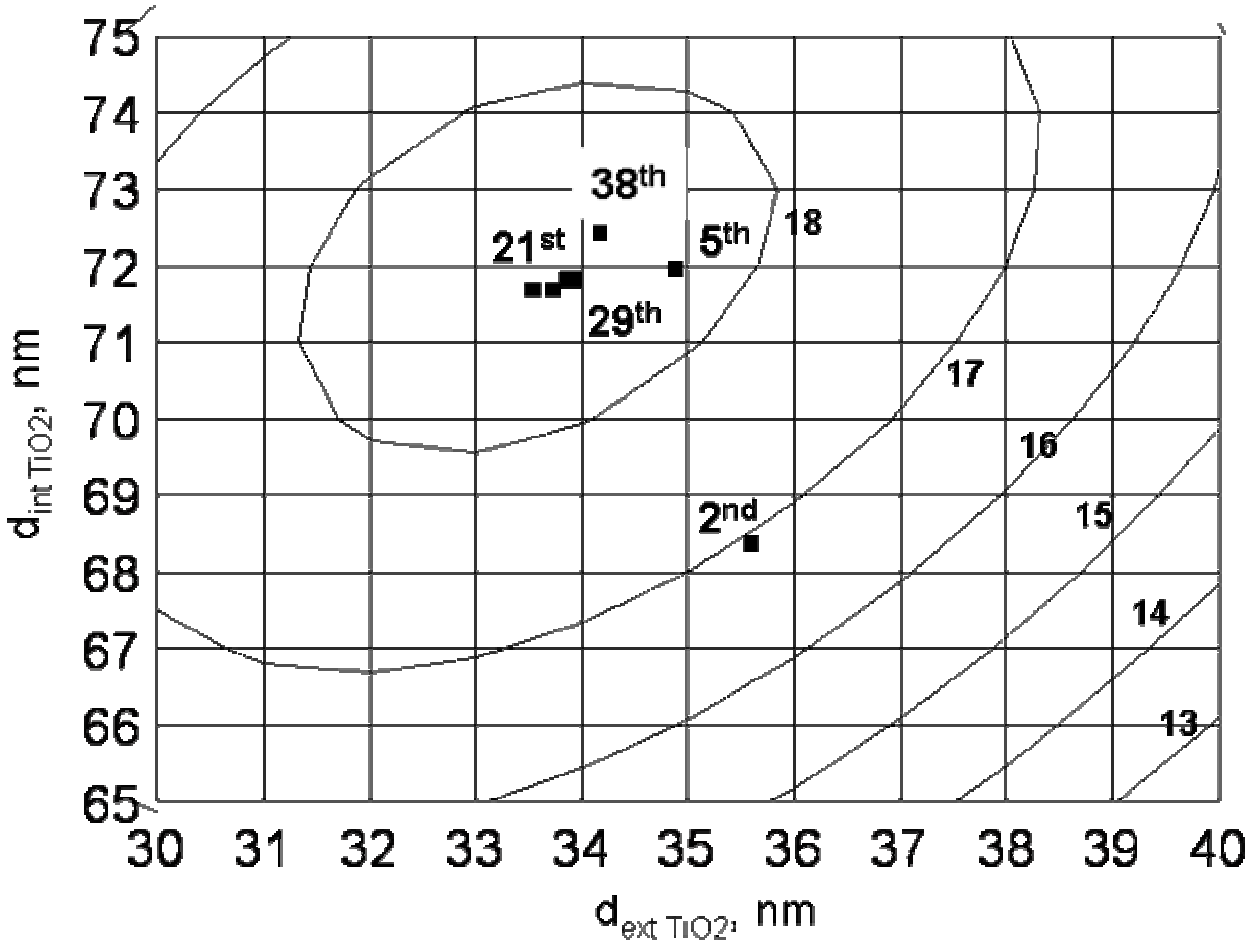

Fig. 8 - R. Li Voti

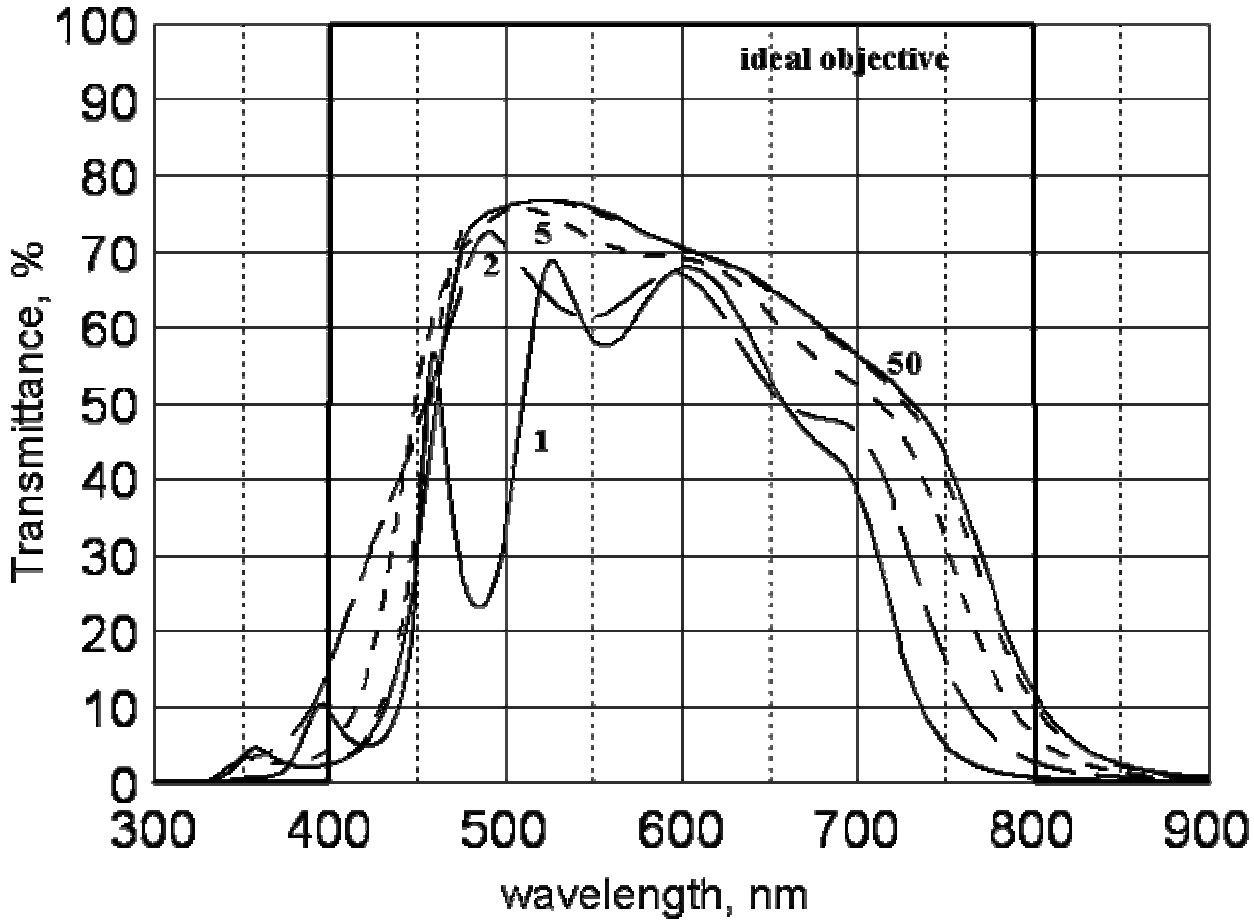

Fig. 9 - R. Li Voti

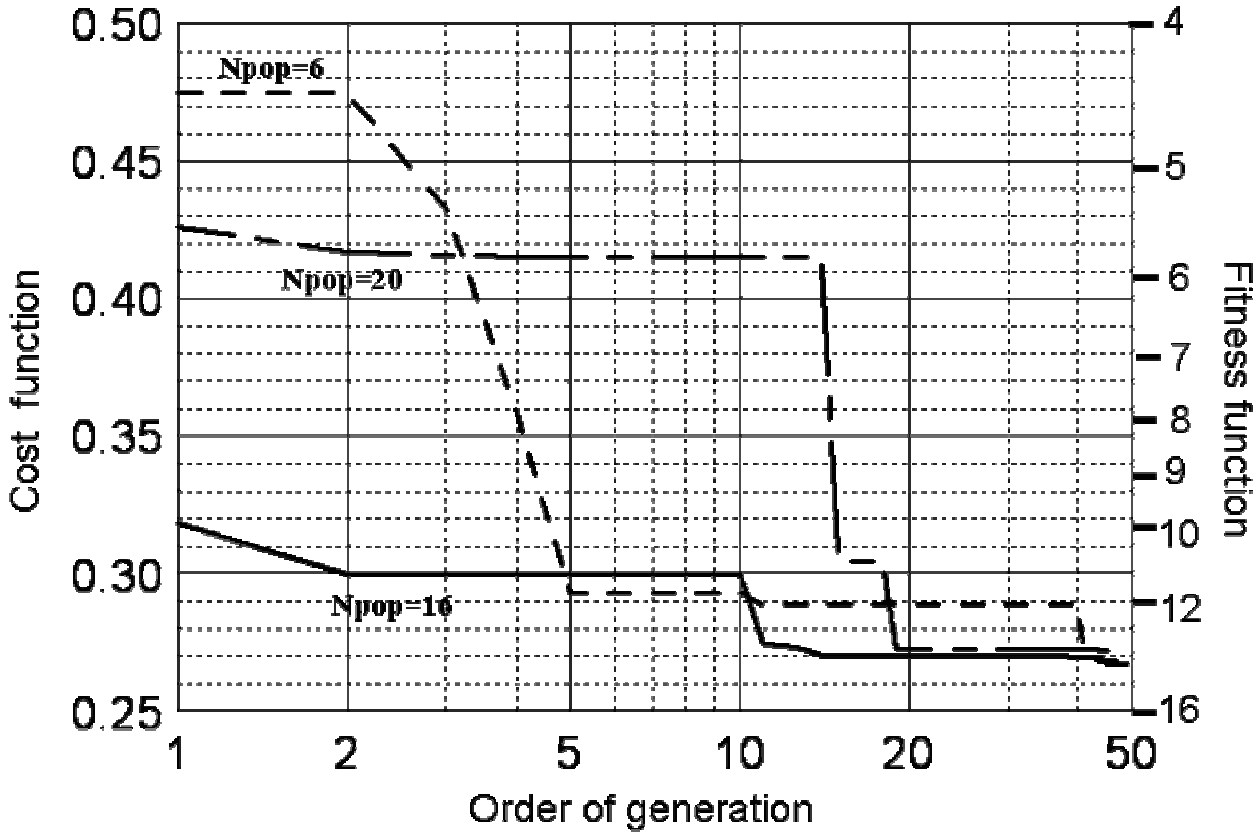

Fig. 10a - R. Li Voti

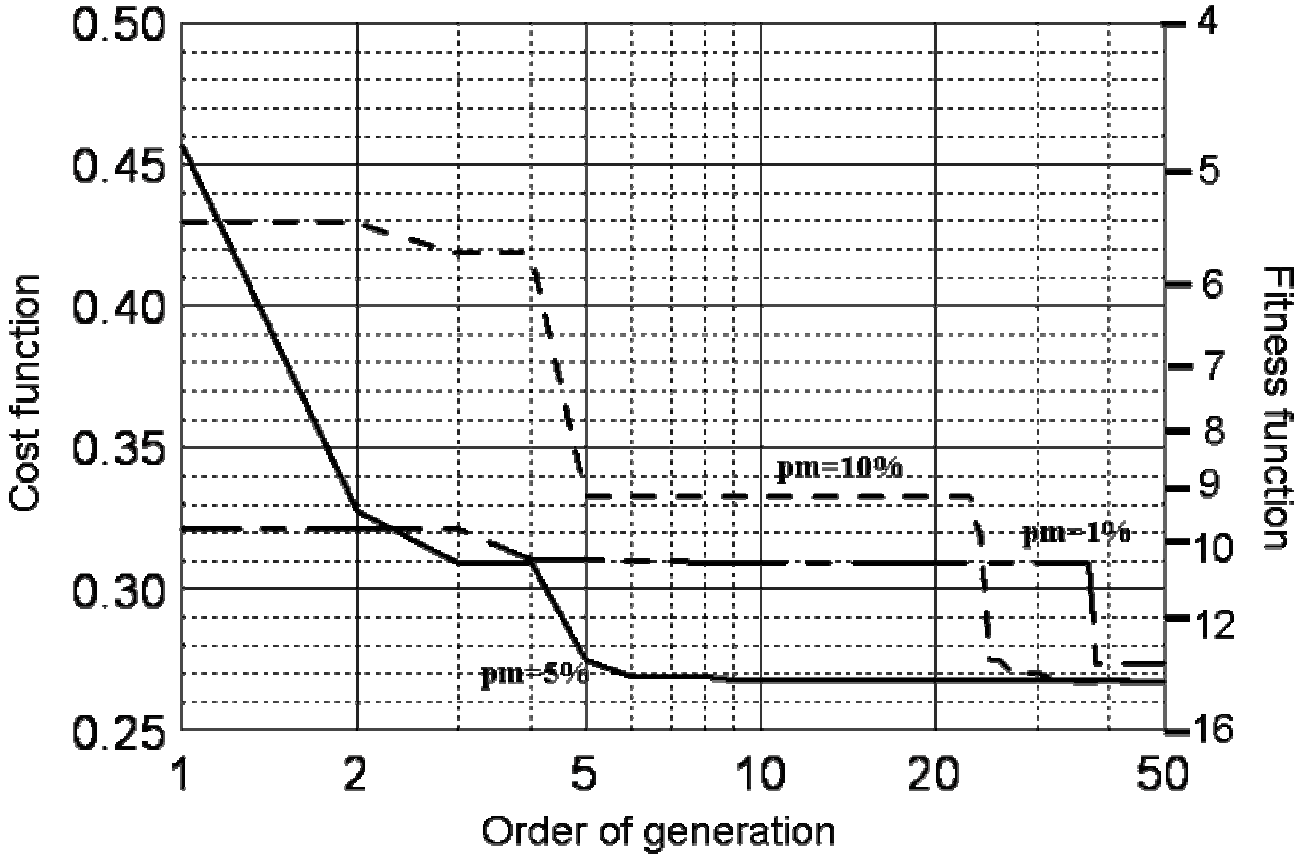

Fig. 10b - R. Li Voti

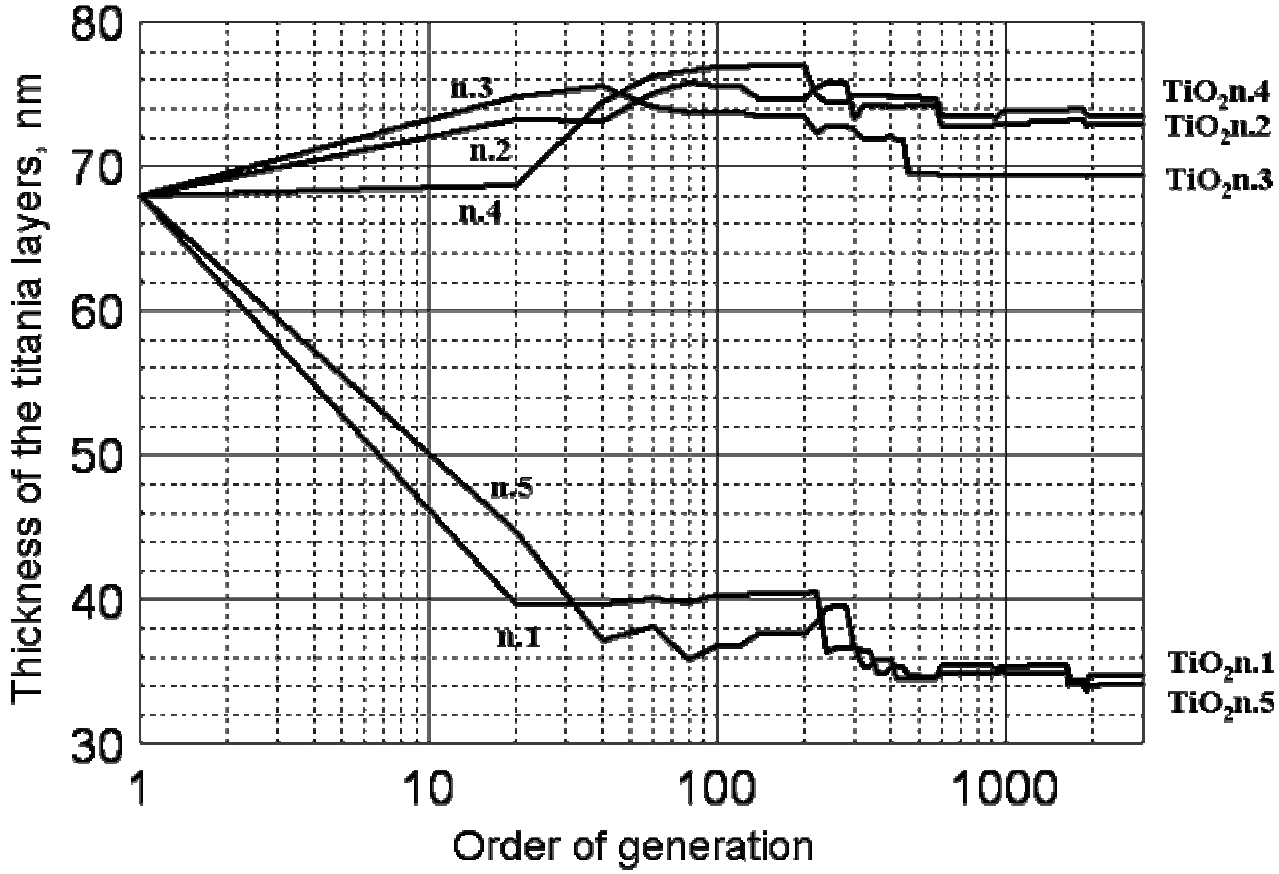

Fig. 11a - R. Li Voti

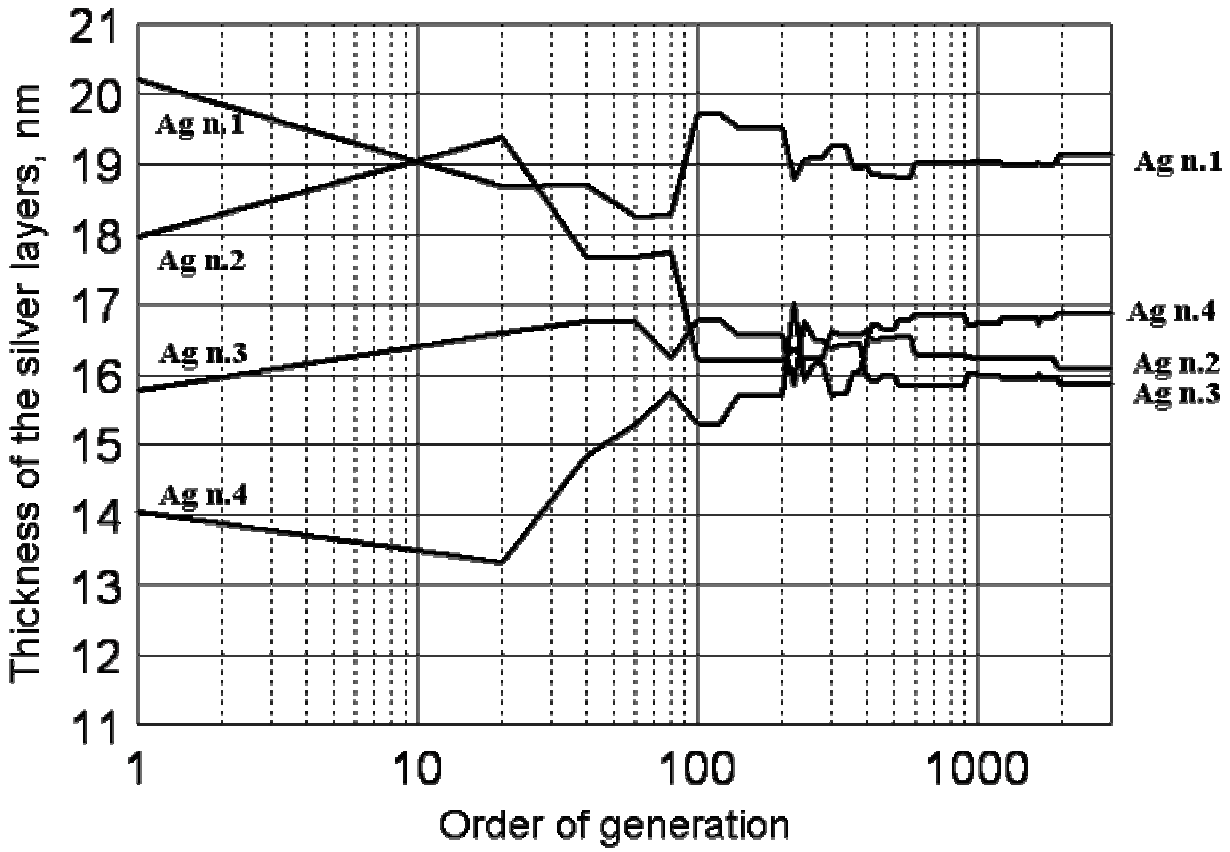

Fig. 11b - R. Li Voti

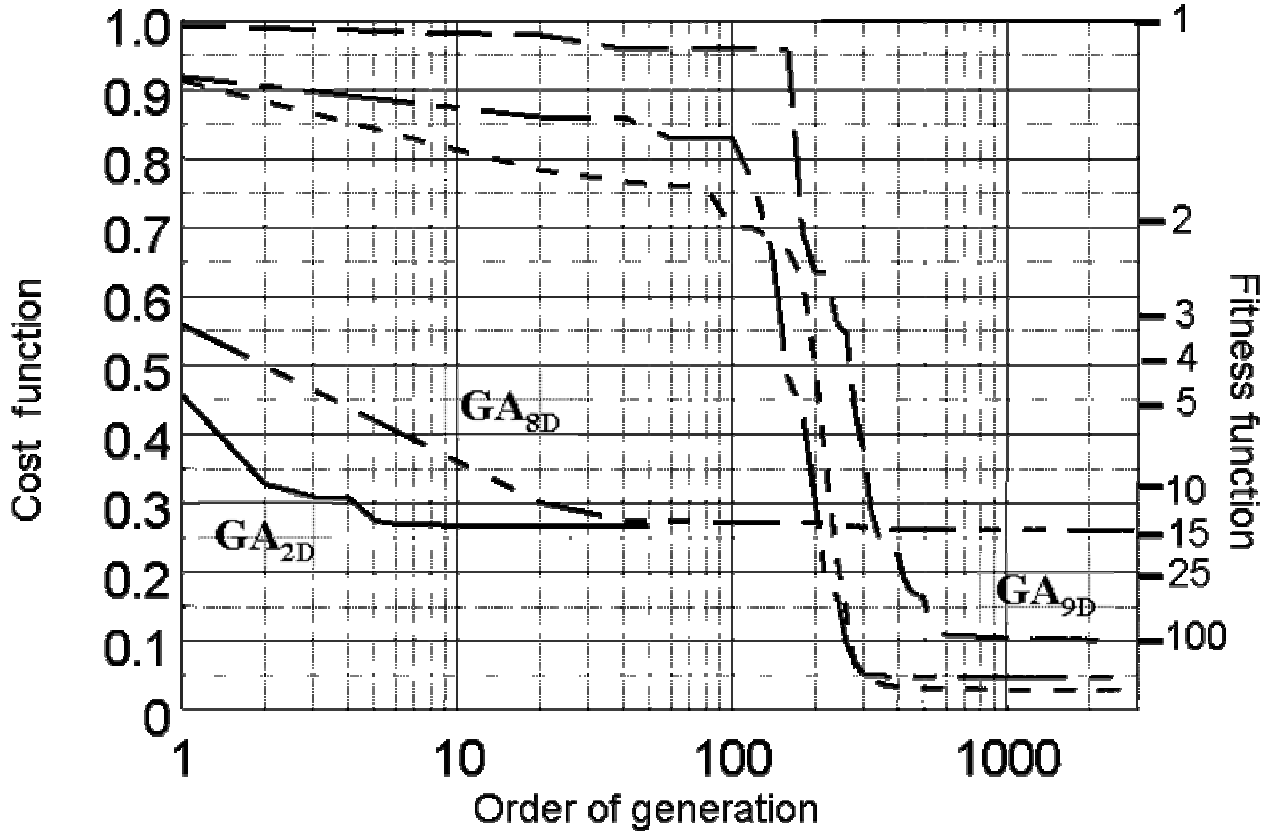

Fig. 12 - R. Li Voti

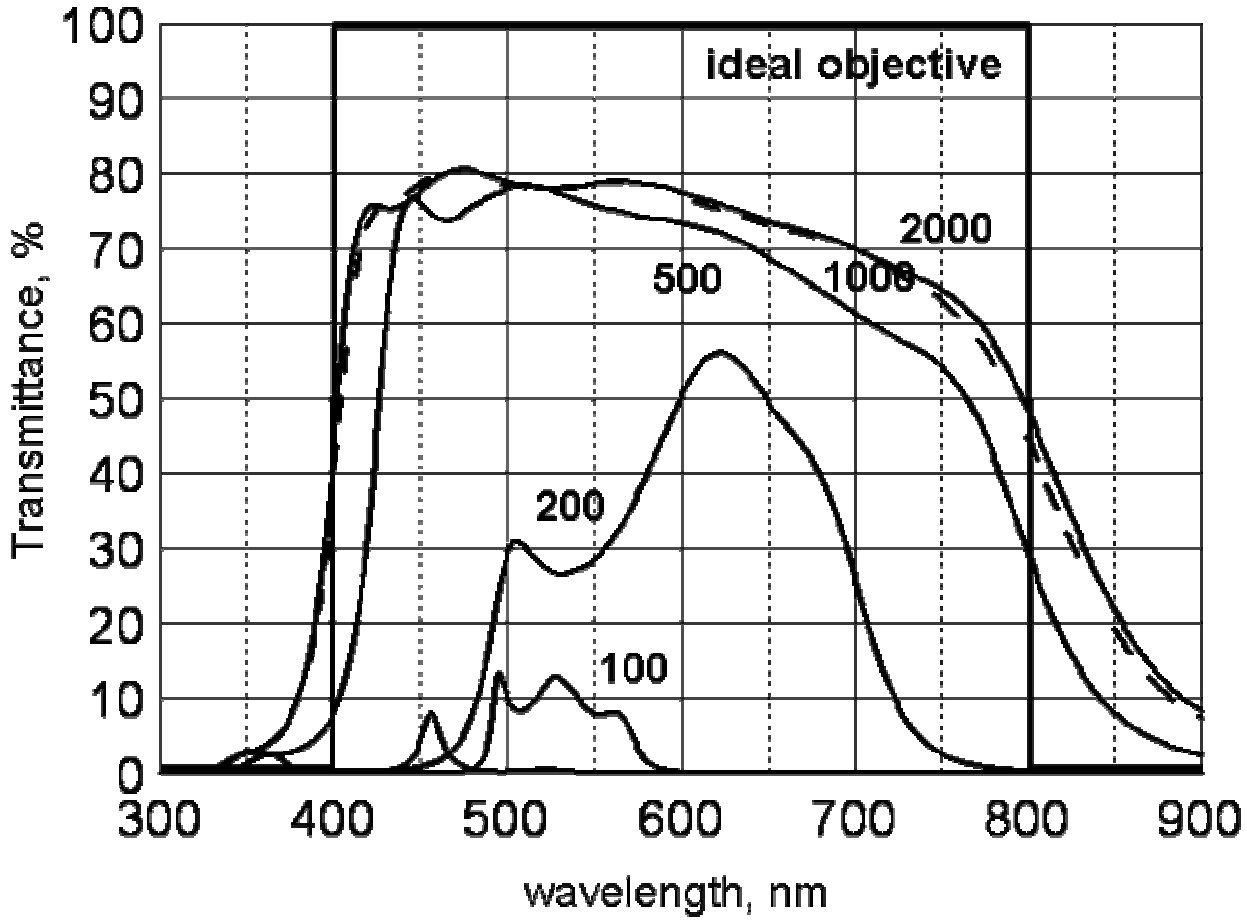

Fig. 13 - R. Li Voti

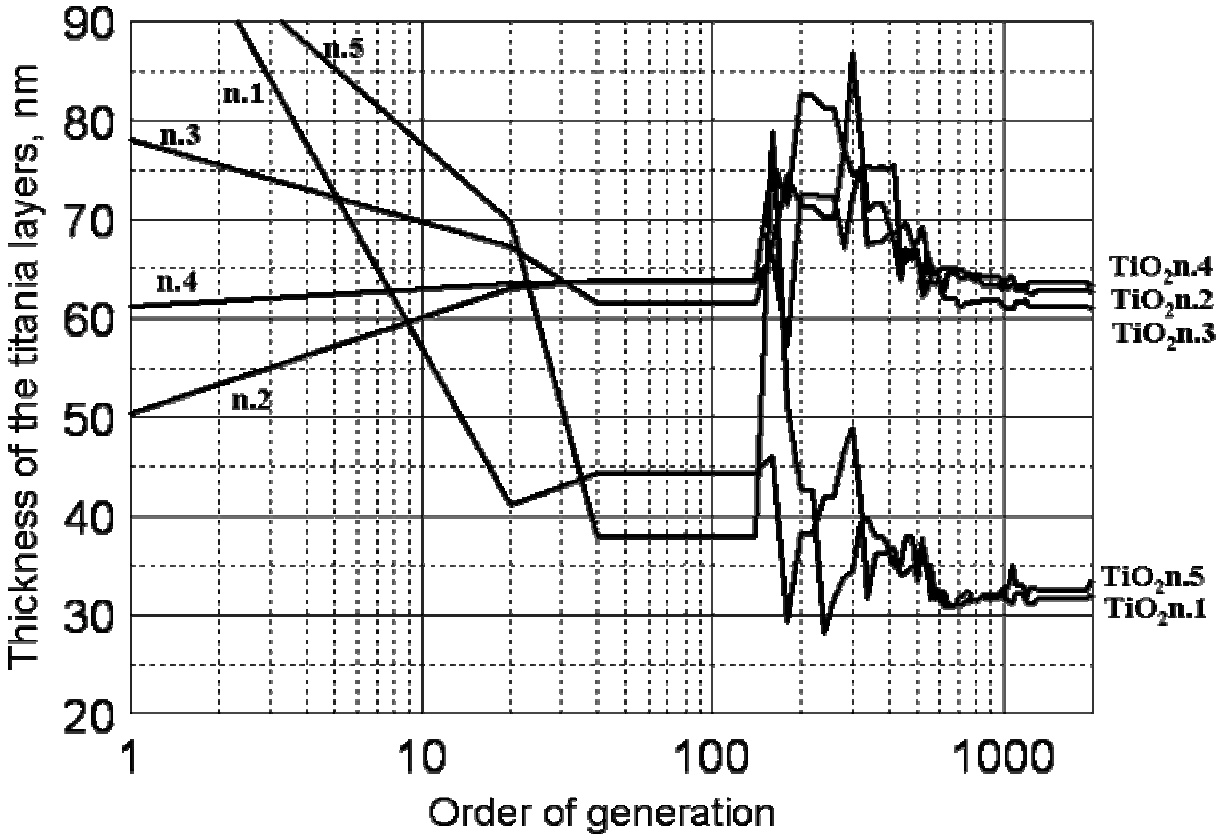

Fig. 14a - R. Li Voti

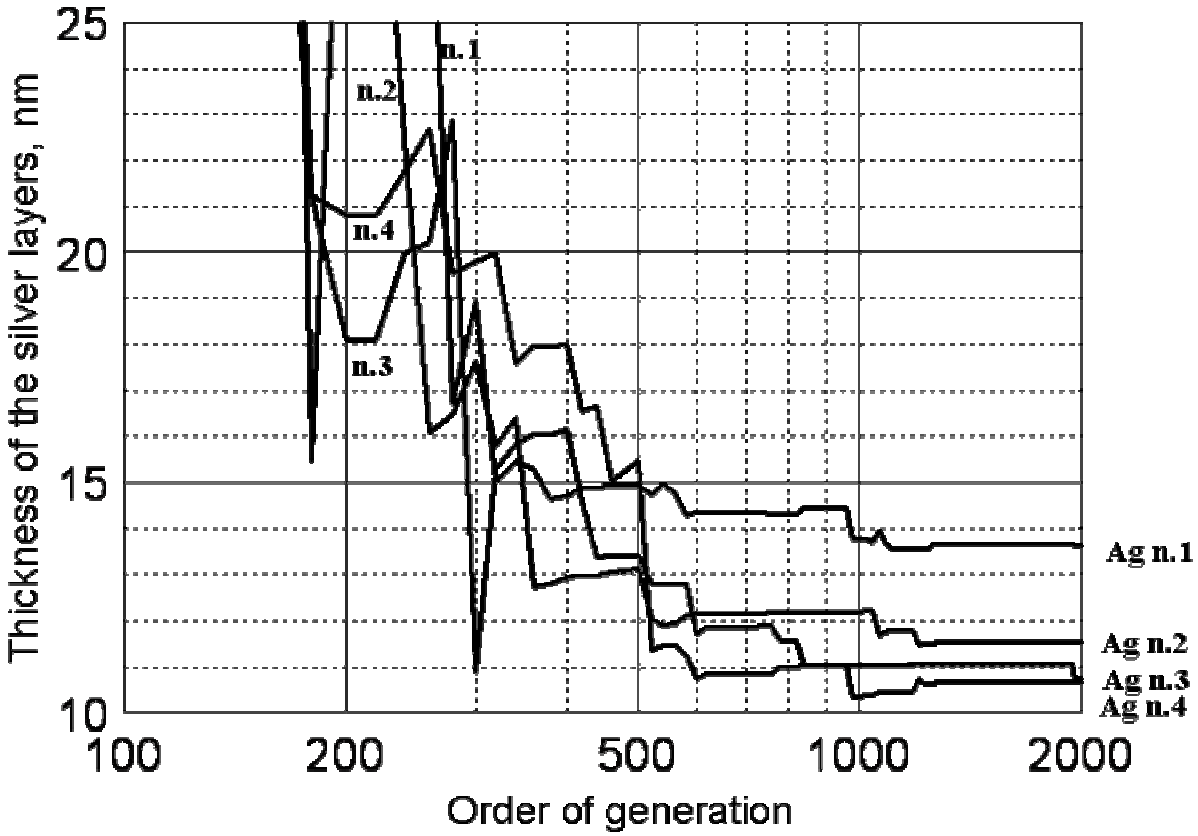

Fig. 14b - R. Li Voti